Published in final edited form as:
Circulation. 2009 March 17; 119(10): 1398–1407. doi:10.1161/CIRCULATIONAHA.108.790501.

Resolution of Established Cardiac Hypertrophy and Fibrosis and Prevention of Systolic Dysfunction in a Transgenic Rabbit Model of Human Cardiomyopathy Through Thiol-Sensitive Mechanisms

Raffaella Lombardi, MD, PhD[1], **Gabriela Rodriguez, MD**[1], **Suet Nee Chen, MS**[2], **Crystal M. Ripplinger, PhD**[4], **Wenwen Li, PhD**[4], **Junjie Chen, PhD**[4], **James T. Willerson, MD**[1], **Sandro Betocchi, MD**[3], **Samuel A. Wickline, MD**[4], **Igor R. Efimov, PhD**[4], and **Ali J. Marian, MD**[1]

[1] Center for Cardiovascular Genetics, Brown Foundation Institute of Molecular Medicine, University of Texas Health Science Center, and Texas Heart Institute, Houston

[2] Baylor College of Medicine, Houston, Tex

[3] Department of Clinical Medicine, Cardiovascular and Immunological Sciences, Federico II University of Naples, Naples, Italy

[4] Department of Biomedical Engineering, Washington University in St Louis, St Louis, Mo

Abstract

Background—Cardiac hypertrophy, the clinical hallmark of hypertrophic cardiomyopathy (HCM), is a major determinant of morbidity and mortality not only in HCM but also in a number of cardiovascular diseases. There is no effective therapy for HCM and generally for cardiac hypertrophy. Myocardial oxidative stress and thiol-sensitive signaling molecules are implicated in pathogenesis of hypertrophy and fibrosis. We posit that treatment with *N*-acetylcysteine, a precursor of glutathione, the largest intracellular thiol pool against oxidative stress, could reverse cardiac hypertrophy and fibrosis in HCM.

Methods and Results—We treated 2-year-old β-myosin heavy-chain Q403 transgenic rabbits with established cardiac hypertrophy and preserved systolic function with *N*-acetylcysteine or a

Correspondence to Ali J. Marian, MD, Center for Cardiovascular Genetics, 6770 Bertner St, DAC 900A, Houston, TX 77030. Ali.J.Marian@uth.tmc.edu.

The online-only Data Supplement is available with this article at http://circ.ahajournals.org/cgi/content/full/CIRCULATIONAHA.108.790501/DC1.

Disclosure
None.

CLINICAL PERSPECTIVE
Hypertrophic cardiomyopathy (HCM) is a genetic disease characterized by primary cardiac hypertrophy. Cardiac hypertrophic and accompanying fibrosis are major determinants of clinical outcomes, including the risk of sudden cardiac death, not only in patients with HCM but also in patients with various cardiovascular diseases. Current pharmacological agents are not known to reverse established cardiac hypertrophy and fibrosis in patients with HCM. We and others have proposed that cardiac hypertrophy and fibrosis in HCM are secondary to activation of various stress-responsive signaling and trophic molecules, including oxidative stress-responsive molecules. Hence, cardiac hypertrophy and fibrosis are potentially reversible. We show in a transgenic rabbit model of human HCM that long-term treatment with *N*-acetylcysteine (NAC), a precursor of glutathione, the largest intracellular thiol pool against oxidative stress in the body, reverses established cardiac hypertrophy and fibrosis. We show that treatment with NAC also prevents deterioration of cardiac systolic function and reduces susceptibility to arrhythmias. We document the beneficial effects of NAC at molecular, cellular, and whole organ levels and illustrated putative molecular mechanisms. The findings suggest the potential utility of NAC in treatment of patients with HCM, a major cause of sudden cardiac death in the young and an important determinant of morbidity in the elderly. Because cardiac hypertrophy, fibrosis, and systolic dysfunction are common to various cardiovascular diseases, the findings could have broader clinical implications. Clinical studies are needed to determine the potential beneficial effects of NAC in prevention and treatment of HCM and heart failure in humans.

placebo for 12 months (n = 10 per group). Transgenic rabbits in the placebo group had cardiac hypertrophy, fibrosis, systolic dysfunction, increased oxidized to total glutathione ratio, higher levels of activated thiol-sensitive active protein kinase G, dephosphorylated nuclear factor of activated T cells (NFATc1) and phospho-p38, and reduced levels of glutathiolated cardiac α-actin. Treatment with *N*-acetylcysteine restored oxidized to total glutathione ratio, normalized levels of glutathiolated cardiac α-actin, reversed cardiac and myocyte hypertrophy and interstitial fibrosis, reduced the propensity for ventricular arrhythmias, prevented cardiac dysfunction, restored myocardial levels of active protein kinase G, and dephosphorylated NFATc1 and phospho-p38.

Conclusions—Treatment with *N*-acetylcysteine, a safe prodrug against oxidation, reversed established cardiac phenotype in a transgenic rabbit model of human HCM. Because there is no effective pharmacological therapy for HCM and given that hypertrophy, fibrosis, and cardiac dysfunction are common and major predictors of clinical outcomes, the findings could have implications in various cardiovascular disorders.

Keywords

antioxidants; cardiomyopathy; fibrosis; genetics; hypertrophy

Cardiac hypertrophy is a common response of the heart to stress, whether internal, such as a genetic mutation, or external, such as an increased load. Cardiac hypertrophy, regardless of the etiology or ethnic background, is associated with increased morbidity and mortality, including sudden cardiac death.[1–3] Cardiac hypertrophy is also a major determinant of diastolic heart failure, a common form of heart failure particularly in the elderly.[4] Elucidation of the molecular pathogenesis of cardiac hypertrophy and its reversal through interventions could impart considerable clinical impact in a diverse array of cardiovascular diseases.[5]

Hypertrophic cardiomyopathy (HCM) is genetic paradigm of cardiac hypertrophic response. HCM is diagnosed clinically by cardiac hypertrophy in the absence of an external cause and pathologically by myocyte hypertrophy, disarray, and interstitial fibrosis. Cardiac hypertrophy and fibrosis are major determinants of clinical outcome, including the risk of sudden cardiac death in HCM.[3,6] The molecular genetic basis of HCM is partially known, and more than a dozen causal genes are identified.[7] Mechanistic studies point to diversity of the initial functional defects imparted by the causal mutations (reviewed in Reference 7). The functional defects encompassing changes in Ca^{2+} sensitivity of myofibrillar ATPase activity, force generation, and actomyosin cross-bridge kinetics provide the stimulus for expression of cardiac hypertrophy (reviewed in Reference 7). Thus, cardiac hypertrophy is a secondary phenotype and therefore is potentially reversible.

To elucidate the molecular pathogenesis of HCM, we have generated β-myosin heavy chain (MyHC)-Q403 transgenic rabbits, which recapitulate the phenotype of human HCM.[8–10] We have shown the potential to prevent and reverse cardiac phenotype in the β-MyHC-Q403 rabbits through pharmacological interventions.[11,12] Likewise, we have shown increased levels of myocardial lipid peroxides, markers of oxidative stress, in β-MyHC-Q403 transgenic rabbits.[12] Moreover, we and others have implicated oxidative stress and thiol-sensitive mechanisms in the pathogenesis of fibrosis in various conditions.[13–15] However, the potential salutary effect of modulating the thio-sensitive pathways on cardiac hypertrophy, the clinical hallmark of HCM, remains to be determined. We performed a placebo-controlled study and treated the β-MyHC-Q403 transgenic rabbits exhibiting cardiac hypertrophy with either a placebo or *N*-acetylcysteine (NAC), a precursor to glutathione, the largest intracellular thiol pool, for 1 year and delineated the effects on cardiac phenotype at organ, cellular, and molecular levels.

Methods

We provide an expanded version of Methods in the online-only Data Supplement. The investigation conforms to the *Guide for the Care and Use of Laboratory Animals* published by the US National Institutes of Health and was approved by the Institutional Animal Care and Use Committee.

β-MyHC-Q403 Transgenic Rabbits

Adult transgenic rabbits exhibit cardiac hypertrophy, interstitial fibrosis, myocyte disarray, and preserved global systolic function but systolic dysfunction on aging, as published.[8–10]

Placebo-Controlled Study and Administration of NAC

We treated age-, sex-, and body weight–matched adult *β*-MyHC-Q403 transgenic rabbits with either a placebo (drinking water) or NAC (500 mg/kg per day; Sigma-Aldrich, St Louis, Mo) for 12 months (n = 10 per group). The dose was selected on the basis of prior data.[13,14,16] We included 10 matched nontransgenic rabbits as controls. The primary end point of the study was change in left ventricular (LV) mass corrected for body weight over the study period. The secondary end points were changes in other echocardiographic indices of cardiac hypertrophy and function as well as changes in histological phenotype.

Blood and Myocardial Levels of Oxidized and Total Glutathione

We measured plasma (n = 6 rabbits per group) and myocardial (n = 3 per group) levels of oxidized glutathione (GSSG) and total glutathione (reduced glutathione [GSH] plus GSSG) by a spectrophotometric method using a commercially available kit (catalog No. 371757, Calbiochem, Darmstadt, Germany) per the manufacturer's instructions.

M-Mode, 2-Dimensional, and Doppler Echocardiography

We performed and analyzed echocardiography without knowledge of the group assignment or genotypes as published.[9–12]

Myocyte Cross-Sectional Area, Collagen Volume Fraction, and Myocyte Disarray

We measured myocyte cross-sectional area, collagen volume fraction (CVF), and myocyte disarray by semiautomated planimetry in age-, sex-, and body weight–matched nontransgenic and transgenic rabbits, as published with modest modifications.[9–12] We performed the analysis without knowledge of the genotypes and group assignment and established reproducibility by repeating the measurements in 20 to 40 randomly selected sections.

Diffusion-Weighted Magnetic Resonance Imaging

We performed diffusion-weighted magnetic resonance imaging (MRI) on 3.7% formaldehyde-perfused hearts as published.[17,18] We calculated myofiber helix angle (α) for a mid LV short-axis slice at 10 steps across the LV wall from epicardium to endocardium in four 20°-wide sectors at the anterior, lateral, inferior, and septal regions. We calculated the fiber angle for the entire slice as the average of these regions.

Thiol-Sensitive Signaling Kinases and Phosphatases

We determined levels of active (dephosphorylated) nuclear factor of activated T cells (NFATc) in cardiac nuclear proteins extracts by enzyme-linked immunosorbent assay. The assay is based on binding of nuclear protein extracts to oligonucleotides containing NFATc consensus binding site (5-AGGAAA-3′) and detection with the use of an antibody against an accessible epitope on nuclear factor of activated T cells 1 (NFATc1). We determined active cGMP-dependent

protein kinase (PKG) levels by enzyme-linked immunosorbent assay on the basis of detection of phosphorylation of a specific substrate. We detected and quantified expression levels of total and phosphorylated ERK 1/2, p38, and Jun N-terminal kinases (JNK) 54/46 by immunoblotting using pan-specific and phospho-specific antibodies.

Glutathiolated Cardiac α-Actin

We detected and quantified glutathiolation of cardiac α-actin by coimmunoprecipitation under nonreducing conditions. We precipitated cardiac α-actin in total protein extracts by adding anti-cardiac α-actin antibody and detected glutathiolated cardiac α-actin by immunoblotting using a mouse monoclonal anti-GSH antibody.

Nuclear G-Actin

We stained thin myocardial sections with a fluorescent conjugate of bovine pancreatic DNase 1, an established marker for monomeric (G) actin.[19] The sections were washed and mounted in fluorescence mounting medium containing 4′,6-diamidino-2-phenylindole (DAPI). We quantified the number of positively stained myocytes in 1000 myocytes per rabbit.

Subcellular Fractionation of Cardiac α-Actin

We extracted nuclear and cytosolic proteins per a published protocol.[20] We collected the cytosolic and nuclear protein fraction by homogenization of minced heart tissues in buffers containing 250 mmol/L and 2 mol/L sucrose, respectively, and through a series of centrifugations and filtrations. Likewise, we extracted membrane and cytoskeletal proteins through a series of homogenization of minced heart tissues and centrifugation in buffers containing NP-40 or PIPES, respectively.

Protein Degradation

We analyzed protein degradation by assessing calpains 1/2 and the 20S proteasome activities by fluorometric assays based on the detection of the fluorophore 7-amino-4-methylcoumarin (AMC). AMC is released on cleavage from Suc-LLVY-AMC in the presence of calpain-containing samples, Ca^{2+}, and a reducing agent or in the presence of 20S proteasome and its activator (SDS). We performed the assays in the presence of specific activators and inhibitors and measured free AMC levels. We determined the proteolytic activities by subtracting the activity obtained in the presence of inhibitors from the activity detected with the activators.

Optical Mapping

We mapped the entire anterior epicardial surface of the heart using a 16×16 photodiode array with a field of view of ≈2.7×2.7 cm, as published.[17] To suppress the motion artifacts, we added excitation-contraction uncoupler 2,3-butanedione monoxime to the perfusate. We injected voltage-sensitive dye di-4-ANEPPS diluted in dimethylsulfoxide into hearts and paced the hearts. We determined the effective refractory period as the last S2 interval to capture using an S1-S2 protocol with S2 delivered at decremental intervals.

To determine the vulnerable grid, we applied a train of 20 paced beats at a basic cycle length of 300 ms followed by a truncated exponential monophasic shock at a specified coupling interval. We defined sustained arrhythmias as arrhythmias lasting >6 shock-induced extra beats. The upper and lower limits of vulnerability were the highest and lowest shock strengths to induce a sustained arrhythmia, respectively.

Statistical Analysis

We expressed the continuous variables as mean±SD. We compared differences among the continuous variables that satisfied the normality distribution by 1-way ANOVA and applied

the Bonferroni correction to multiple comparison tests. Variables that were not normally distributed were compared by Kruskal-Wallis test. We compared the differences between the baseline and follow-up continuous variables by paired *t* test. Differences in the categorical variables were analyzed by χ^2 test. All statistical analyses were performed with the use of STATA version 9.2.

The authors had full access to and take responsibility for the integrity of the data. All authors have read and agree to the manuscript as written.

Results

Baseline (Before Treatment) Characteristics

The data are shown in Table 1. The mean age, body weight, and male/female ratio were similar (matched) in the experimental groups. The mean interventricular septal thickness, posterior wall thickness, LV mass, and LV mass indexed to body weight (LV mass/body weight) were greater in transgenic than in nontransgenic rabbits. We detected no significant differences in indices of cardiac hypertrophy and function, including LV fractional shortening (LVFS) between transgenic rabbits in the placebo and NAC groups before treatment.

GSSG/GSSG+GSH Ratio

GSSG/GSSG+GSH ratio in the blood was increased in transgenic rabbits in the placebo group by >2-fold compared with nontransgenic rabbits (Figure 1A). In contrast, in the NAC group, it was comparable to that in the nontransgenic rabbits but significantly less than that in the placebo group. Likewise, myocardial GSSG/GSSG+GSH ratio was increased by 3-fold in the placebo group compared with nontransgenics (Figure 1B). In contrast, the ratio in the NAC group was comparable to that in the nontransgenic rabbits.

Cardiac Hypertrophy and Function

Echocardiographic indices of cardiac hypertrophy were either increased or unchanged in the placebo group at 12-month follow-up compared with baseline (Table 1). In contrast, all echocardiographic indices of cardiac hypertrophy were regressed to normal values after 12-month treatment with NAC.

LVFS was reduced significantly in transgenic rabbits in the placebo group at the follow-up (Table 1). In contrast, LVFS was unchanged in the nontransgenic rabbits and was modestly increased in transgenic rabbits treated with NAC. Changes in the LV end-systolic diameter were in accord with changes in LVFS. Concordant with decreased LVFS in the placebo group, mitral valve inflow E/A, an index of LV filling pressure, was increased and isovolumic relaxation time was decreased significantly (Table 1). In contrast, these indices were unchanged in the nontransgenic or transgenic rabbits treated with NAC.

Myocyte Hypertrophy and Interstitial Fibrosis

Corroborating the echocardiographic indices of cardiac hypertrophy, myocyte cross-sectional area was increased by ≈20% in transgenic rabbits in the placebo group compared with the nontransgenic group (Figure 2). In contrast, myocyte cross-sectional area in the NAC group was comparable to that in the nontransgenic rabbits. The mean number of myocytes per each microscopic field (×400) was lower in the placebo group compared with nontransgenic rabbits or the NAC group (Figure 2). The reproducibility of the measurements of myocyte cross-sectional area, determined by calculating the intraobserver variability, was 3.5%. The correlation between the first and second measurements of myocyte cross-sectional area was 0.881.

CVF was increased by ≈3-fold in the placebo group compared with the nontransgenic group (Figure 2). CVF was normal in rabbits treated with NAC. We tested the reproducibility of the measurements in 2 independent settings. The correlation and the mean difference between the 2 independent measurements were 0.94 and 0.20%, respectively (intraobserver variability, 2.29%).

Myocyte Disarray and Myofiber Angle Orientation

Myocyte disarray comprised ≈6% of the myocardium in the nontransgenic rabbits. It was increased by ≈3-fold in the placebo and NAC groups (15% and 18%, respectively; Figure 2). The correlation and the mean difference between the 2 independent measurements were 0.79 and 1.2%.

To complement the results of histological assessment of myocyte disarray, we determined myofibrillar α-helical angle by diffusion-weighted MRI (Figure 3). At the endocardium, myofiber orientation diverged between the transgenic and non-transgenic rabbits but not between the transgenic rabbits in the placebo and NAC groups ($P = 0.036$). However, myofiber α-helix angle at the epicardium differed modestly between transgenic rabbits in the placebo and NAC groups ($P = 0.074$). The overall fiber orientation angle differed only between the nontransgenic and transgenic rabbits in the placebo group ($P = 0.039$) but not between placebo and NAC groups.

Myocardial Levels of Selected Thiol-Sensitive Signaling Kinases and Phosphatase

To gain insight into molecular mechanisms of the beneficial effects of NAC, we determined myocardial levels of selected thiol-sensitive signaling molecules. Protein threonine phosphatases are thiol-sensitive proteins.[21] We measured myocardial levels of dephosphorylated NFATc1, a downstream signal transducer of protein phosphatase 2A calcineurin.[22] We detected 64% increase in active NFATc1 levels in the placebo group compared with nontransgenic rabbits (Figure 4A). Myocardial levels of NFATc1 in the NAC group were comparable to levels in the nontransgenic group but 2-fold lower than levels in the placebo group.

Likewise, myocardial levels of PKG, a cysteine redox sensor known to be activated by oxidative stress,[23] were increased by ≈80% in the placebo group compared with the nontransgenic group ($P<0.001$). Myocardial levels of active PKG were normal in rabbits treated with NAC and comparable to nontransgenic controls (Figure 4B).

Myocardial levels of phospho-p38 kinase were increased in the transgenic rabbits in the placebo group but were normal in the NAC-treated group (Figure 4C and 4D). There were modest changes in myocardial levels of phosphorylated ERK1/2 and JNK 54/46 among the groups (data not shown).

Glutathiolation of Cardiac α-Actin

Cytoskeletal proteins, particularly α-actin, are subject to glutathiolation, a modification that could affect cell cytoskeletal organization and mobility, actin polymerization, and its nuclear localization.[24] Myocardial levels of glutathiolated cardiac α-actin were lower by 35% in the placebo group compared with nontransgenic rabbits but were normal in the NAC-treated rabbits (Figure 5), which paralleled changes in the GSSG/GSSG+GSH ratio.

Nuclear G-Actin—Because glutathiolation of actin could affect polymerization of monomeric (G) actin to F-actin and because G-actin interacts with prohypertrophic serum response factor,[25,26] we determined the effects of NAC on nuclear localization of G-actin (Figure 5C). The percentage of positively stained myocytes was not significantly different

among the groups (nontransgenic, 0.75±0.20%; placebo, 0.69±0.13%; NAC, 0.81±0.21%; $P = 0.676$).

Subcellular Localization of Cardiac α-Actin

To determine whether glutathiolation of α-actin altered sub-cellular localization of α-actin, we detected levels of cardiac α-actin in cytosolic, nuclear, membrane, and cytoskeletal protein extracts by immunoblotting. There were modest but not nonsignificant differences in α-actin levels in each subcellular fraction among the groups (Figure 5D, 5E, 5F and Figure I in the online-only Data Supplement).

Protein Degradation—Because proteolytic activities of proteasome and cysteine proteases are also influenced by reduced sulfhydryls,[27] we measured activities of calpains 1 and 2 and 20S proteasome in the myocardial extracts. We detected no significant differences in activity levels of 20S proteosome or calpains 1 and 2 among the groups (Figure II in the online-only Data Supplement).

Reduced Vulnerability to Ventricular Arrhythmias

To determine the potential effects of regression of cardiac hypertrophy on arrhythmogenic propensity, we determined vulnerability to ventricular arrhythmias by optical mapping. The upper limits of vulnerability of both ventricles were increased by ≈2-fold in the placebo group compared with the nontransgenic group, but the lower limits were unchanged (Table 2). The upper limits of vulnerability, vulnerable window, and vulnerable period were significantly lower in the NAC group compared with placebo (Figure 6A and 6B). NAC had no detrimental effects on any of the electrophysiological parameters measured.

Discussion

We showed that long-term treatment with NAC, a precursor to the most abundant intracellular nonprotein thiol pool against oxidative stress,[28] reversed cardiac and myocyte hypertrophy and interstitial fibrosis, prevented LV systolic dysfunction, and improved arrhythmogenic propensity in an established transgenic rabbit model of human HCM.[8–10,12] Reversal of the phenotype was associated with normalization of levels of oxidized glutathione; glutathiolated cardiac α-actin; and thiol-sensitive molecules active PKG, calcineurin target NFATc1, and phospho-p38. Treatment with NAC did not affect myocyte or myofibrillar organization or subcellular localization of α-actin and G-actin. The antifibrotic effect of NAC is in accord with the findings in other models and organs.[13,29–33] Resolution of cardiac and myocyte hypertrophy and prevention of cardiac systolic dysfunction with NAC are novel findings. The data suggest the potential beneficial effects of this safe prodrug in reversal of cardiac phenotype in HCM and prevention of global cardiac systolic dysfunction.

NAC provides the cysteine necessary for GSH synthesis. Accordingly, glutamate cysteine ligase (γ-glutamylcysteine synthetase) catalyzes binding of cysteine to glutamate to generate γ-glutamylcysteine. Then glutathione synthetase catalyzes binding of glycine to γ-glutamylcysteine to generate GSH (γ-glutamylcysteinylglycine). The transfer of glutamate from GSH to other amino acids by the γ-glutamyl transpeptidase and subsequent catalysis of cysteinylglycine dipeptide to cysteine and glycine by a dipeptidase completes the cycle of synthesis and metabolism. Glutathione reductase catalyzes the recycling of reduced glutathione from oxidized glutathione. NAC by providing cysteine replenishes GSH, which is usually depleted in disease states, as was also found in the β-MyHC-Q403 rabbits. The finding is in accord with our previous data showing increased levels of markers of oxidative stress in this model.[12] Increased GSSG/GSSG+GSH in the β-MyHC-Q403 rabbits was associated with changes in activities of selected thiol-sensitive kinases and calcineurin phosphatase involved

in cardiac hypertrophy and function. A notable effect of NAC was reduction of prohypertrophic dephosphorylated NFATc1 levels, which provides a plausible molecular mechanism for the antihypertrophic and antifibrotic effects of NAC.[22] Likewise, myocardial levels of PKG, a cysteine-redox sensor activated on exposure to oxidative stress,[23] were increased in the placebo group but were normal in the NAC group. Reduced myocardial levels of phospho-p38 in the NAC group are consistent with the known inhibitory effect of NAC on p38 activity.[13,28] The changes in levels of active PKG and phospho-p38 may simply reflect the xidative state of the myocardium but necessarily mediate the beneficial effects of NAC on cardiac structure and function. The findings also do not exclude involvement of alternative mechanisms for the salutary effects of NAC in our HCM model. Given the complexity of the molecular biology of cardiac hypertrophy, fibrosis, and dysfunction, the effects could encompass multiple independent and interactive pathways, including transcriptional regulation of gene expression and posttranslational thiol modification of cysteines at the surface of numerous kinases, phosphatases, and sarcomeric proteins.

Actin is a redox-sensitive protein, known to be glutathiolated via formation of a mixed disulfide between cysteine residues and glutathione.[24] The modification is considered essential for its polymerization, cytoskeleton organization, formation of stress fibers, and cell spreading.[24,25] Monomeric or G-actin is an important regulator of the prohypertrophic serum response factor.[26,34] Levels of glutathiolated cardiac α-actin, in accord with increased GSSG/GSSG +GSH, were reduced in the placebo group. However, we found no significant changes in nuclear G-actin levels, a potential antihypertrophic molecule. Thus, the antihypertrophic effect of NAC was independent of nuclear localization of G-actin and serum response factor.[26,34] However, experiments in an in vivo model wherein the stimulus for induction of the phenotype is chronic and modest, compared with in vitro studies, may not offer sufficient resolution to substantiate the biological significance of glutathiolated cardiac α-actin in regression of cardiac phenotype in HCM.

The attractiveness of NAC as a potential therapy for HCM and heart failure is emphasized by its well-established safety profile in humans, even at doses as high as 8 g/d.[35,36] The well-established safety of NAC, along with the convenience of administration and the plurality of its beneficial effects at organ, cellular, and molecular levels, renders NAC a highly attractive therapeutic option for cardiomyopathies. The clinical significance of the findings is highlighted by the fact that there is currently no effective pharmacological therapy for HCM and in general for cardiac hypertrophy. Nonetheless, the findings could be restricted to our specific animal models or the specific mutations and may not be applicable across the spectrum of human HCM. We did not observe a discernible side effect. However, a recent study reported a higher pulmonary artery pressure in mice treated with NAC.[37] In contrast, several studies have shown the beneficial effects of NAC in improving pulmonary artery hypertension.[32,33,38] Moreover, NAC has been used in humans to treat various conditions including idiopathic pulmonary fibrosis without reports of pulmonary hypertension as a side effect.[29] We did not measure pulmonary artery pressure in our rabbits but did not notice changes in pulmonary artery or right ventricular size and function on echocardiograms.

In summary, we have shown that long-term treatment with NAC, a precursor to the most abundant intracellular defense mechanism against oxidative damage, reverses established cardiac hypertrophy and fibrosis, prevents cardiac dysfunction, and reduces susceptibility to ventricular arrhythmia in the β-MyHC-Q403 transgenic rabbit model of human HCM. The beneficial effects were associated with favorable changes in myocardial levels of selective thiol-sensitive kinases and phosphatases. The findings raise the potential utility of NAC for treatment of human HCM, a most common discernible cause of sudden cardiac death in the young and a major cause of mortality and morbidity in the elderly.[6] Because cardiac hypertrophy and fibrosis are common and important determinants of clinical outcomes in

various cardiovascular diseases, the findings could have broader implications. Finally, the effect of NAC on prevention of systolic dysfunction signals its potential utility in prevention and treatment of systolic heart failure. Collectively, the findings provide the prerequisite for testing the potential salutary effects of NAC in treatment and prevention of HCM and heart failure in humans.

Supplementary Material

Refer to Web version on PubMed Central for supplementary material.

Acknowledgments

Sources of Funding

This work was supported in part by grants R01-HL68884 and R01-HL67322 from the National Heart, Lung, and Blood Institute, Clinician-Scientist Award in Translation Research from the Burroughs Wellcome Fund (1005907), and the Greater Houston Community Foundation (TexGen).

References

1. Haider AW, Larson MG, Benjamin EJ, Levy D. Increased left ventricular mass and hypertrophy are associated with increased risk for sudden death. J Am Coll Cardiol 1998;32:1454–1459. [PubMed: 9809962]
2. Levy D, Garrison RJ, Savage DD, Kannel WB, Castelli WP. Prognostic implications of echocardiographically determined left ventricular mass in the Framingham Heart Study. N Engl J Med 1990;322:1561–1566. [PubMed: 2139921]
3. Spirito P, Bellone P, Harris KM, Bernabo P, Bruzzi P, Maron BJ. Magnitude of left ventricular hypertrophy and risk of sudden death in hypertrophic cardiomyopathy. N Engl J Med 2000;342:1778–1785. [PubMed: 10853000]
4. Zile MR, Brutsaert DL. New concepts in diastolic dysfunction and diastolic heart failure, part II: causal mechanisms and treatment. Circulation 2002;105:1503–1508. [PubMed: 11914262]
5. Hill JA, Olson EN. Cardiac plasticity. N Engl J Med 2008;358:1370–1380. [PubMed: 18367740]
6. Maron BJ. Hypertrophic cardiomyopathy: a systematic review. JAMA 2002;287:1308–1320. [PubMed: 11886323]
7. Marian AJ. Genetic determinants of cardiac hypertrophy. Curr Opin Cardiol 2008;23:199–205. [PubMed: 18382207]
8. Marian AJ, Wu Y, Lim DS, McCluggage M, Youker K, Yu QT, Brugada R, DeMayo F, Quinones M, Roberts R. A transgenic rabbit model for human hypertrophic cardiomyopathy. J Clin Invest 1999;104:1683–1692. [PubMed: 10606622]
9. Nagueh SF, Chen S, Patel R, Tsybouleva N, Lutucuta S, Kopelen HA, Zoghbi WA, Quinones MA, Roberts R, Marian AJ. Evolution of expression of cardiac phenotypes over a 4-year period in the beta-myosin heavy chain-Q403 transgenic rabbit model of human hypertrophic cardiomyopathy. J Mol Cell Cardiol 2004;36:663–673. [PubMed: 15135661]
10. Nagueh SF, Kopelen HA, Lim DS, Zoghbi WA, Quinones MA, Roberts R, Marian AJ. Tissue Doppler imaging consistently detects myocardial contraction and relaxation abnormalities, irrespective of cardiac hypertrophy, in a transgenic rabbit model of human hypertrophic cardiomyopathy. Circulation 2000;102:1346–1350. [PubMed: 10993850]
11. Patel R, Nagueh SF, Tsybouleva N, Abdellatif M, Lutucuta S, Kopelen HA, Quinones MA, Zoghbi WA, Entman ML, Roberts R, Marian AJ. Simvastatin induces regression of cardiac hypertrophy and fibrosis and improves cardiac function in a transgenic rabbit model of human hypertrophic cardiomyopathy. Circulation 2001;104:317–324. [PubMed: 11457751]
12. Senthil V, Chen SN, Tsybouleva N, Halder T, Nagueh SF, Willerson JT, Roberts R, Marian AJ. Prevention of cardiac hypertrophy by atorvastatin in a transgenic rabbit model of human hypertrophic cardiomyopathy. Circ Res 2005;97:285–292. [PubMed: 16020756]

13. Marian AJ, Senthil V, Chen SN, Lombardi R. Antifibrotic effects of antioxidant N-acetylcysteine in a mouse model of human hypertrophic cardiomyopathy mutation. J Am Coll Cardiol 2006;47:827–834. [PubMed: 16487852]

14. Tirouvanziam R, Conrad CK, Bottiglieri T, Herzenberg LA, Moss RB, Herzenberg LA. High-dose oral N-acetylcysteine, a glutathione prodrug, modulates inflammation in cystic fibrosis. Proc Ntl Acad Sci 2006;103:4628–4633.

15. Takimoto E, Kass DA. Role of oxidative stress in cardiac hypertrophy and remodeling. Hypertension 2007;49:241–248. [PubMed: 17190878]

16. Williams IA, Allen DG. The role of reactive oxygen species in the hearts of dystrophin-deficient mdx mice. Am J Physiol 2007;293:H1969–H1977.

17. Ripplinger CM, Li W, Hadley J, Chen J, Rothenberg F, Lombardi R, Wickline SA, Marian AJ, Efimov IR. Enhanced transmural fiber rotation and connexin 43 heterogeneity are associated with an increased upper limit of vulnerability in a transgenic rabbit model of human hypertrophic cardiomyopathy. Circ Res 2007;101:1049–1057. [PubMed: 17885214]

18. Chen J, Song SK, Liu W, McLean M, Allen JS, Tan J, Wickline SA, Yu X. Remodeling of cardiac fiber structure after infarction in rats quantified with diffusion tensor MRI. Am J Physiol 2003;285:H946–H954.

19. Hitchcock SE. Actin deoxyroboncuclease I interaction: depolymerization and nucleotide exchange. J Biol Chem 1980;255:5668–5673. [PubMed: 6247341]

20. Cox B, Emili A. Tissue subcellular fractionation and protein extraction for use in mass-spectrometry-based proteomics. Nat Protocols 2006;1:1872–1878.

21. Cross JV, Templeton DJ. Regulation of signal transduction through protein cysteine oxidation. Antioxid Redox Signal 2006;8:1819–1827. [PubMed: 16987034]

22. Molkentin JD. Calcineurin-NFAT signaling regulates the cardiac hypertrophic response in coordination with the MAPKs. Cardiovasc Res 2004;63:467–475. [PubMed: 15276472]

23. Burgoyne JR, Madhani M, Cuello F, Charles RL, Brennan JP, Schroder E, Browning DD, Eaton P. Cysteine redox sensor in PKGIa enables oxidant-induced activation. Science 2007;317:1393–1397. [PubMed: 17717153]

24. Fiaschi T, Cozzi G, Raugei G, Formigli L, Ramponi G, Chiarugi P. Redox regulation of beta-actin during integrin-mediated cell adhesion. J Biol Chem 2006;281:22983–22991. [PubMed: 16757472]

25. Dalle-Donne I, Giustarini D, Colombo R, Milzani A, Rossi R. S-Glutathionylation in human platelets by a thiol-disulfide exchange-independent mechanism. Free Radic Biol Med 2005;38:1501–1510. [PubMed: 15890624]

26. Vartiainen MK, Guettler S, Larijani B, Treisman R. Nuclear actin regulates dynamic subcellular localization and activity of the SRF cofactor MAL. Science 2007;316:1749–1752. [PubMed: 17588931]

27. Demasi M, Silva GM, Netto LE. 20 S proteasome from Saccharomyces cerevisiae is responsive to redox modifications and is S-glutathionylated. J Biol Chem 2003;278:679–685. [PubMed: 12409293]

28. Zafarullah M, Li WQ, Sylvester J, Ahmad M. Molecular mechanisms of N-acetylcysteine actions. Cell Mol Life Sci 2003;60:6–20. [PubMed: 12613655]

29. Demedts M, Behr J, Buhl R, Costabel U, Dekhuijzen R, Jansen HM, MacNee W, Thomeer M, Wallaert B, Laurent F, Nicholson AG, Verbeken EK, Verschakelen J, Flower CDR, Capron F, Petruzzelli S, De Vuyst P, van den Bosch JMM, Rodriguez-Becerra E, Corvasce G, Lankhorst I, Sardina M, Montanari M. IFIGENIA Study Group. High-dose acetylcysteine in idiopathic pulmonary fibrosis. N Engl J Med 2005;353:2229–2242. [PubMed: 16306520]

30. Kopp J, Seyhan H, Muller B, Lanczak J, Pausch E, Gressner AM, Dooley S, Horch RE. N-Acetyl-L-cysteine abrogates fibrogenic properties of fibroblasts isolated from Dupuytren's disease by blunting TGF-beta signalling. J Cell Mol Med 2006;10:157–165. [PubMed: 16563228]

31. Liu RM, Liu Y, Forman HJ, Olman M, Tarpey MM. Glutathione regulates transforming growth factor-{beta}-stimulated collagen production in fibroblasts. Am J Physiol 2004;286:L121–L128.

32. Hoshikawa Y, Ono S, Suzuki S, Tanita T, Chida M, Song C, Noda M, Tabata T, Voelkel NF, Fujimura S. Generation of oxidative stress contributes to the development of pulmonary hypertension induced by hypoxia. J ApplPhysiol 2001;90:1299–1306.

33. Liu DD, Kao SJ, Chen HI. N-Acetylcysteine attenuates acute lung injury induced by fat embolism. Crit Care Med 2008;36:565–571. [PubMed: 18216605]

34. Miralles F, Posern G, Zaromytidou AI, Treisman R. Actin dynamics control SRF activity by regulation of its coactivator MAL. Cell 2003;113:329–342. [PubMed: 12732141]

35. Atkuri KR, Mantovani JJ, Herzenberg LA, Herzenberg LA. N-Acetylcysteine: a safe antidote for cysteine/glutathione deficiency. Curr Opin Pharmacol 2007;7:355–359. [PubMed: 17602868]

36. De Rosa SC, Zaretsky MD, Dubs JG, Roederer M, Anderson M, Green A, Mitra D, Watanabe N, Nakamura H, Tjioe I, Deresinski SC, Moore WA, Ela SW, Parks D, Herzenberg LA. N-Acetylcysteine replenishes glutathione in HIV infection. Eur J Clin Invest 2000;30:915–929. [PubMed: 11029607]

37. Palmer LA, Doctor A, Chhabra P, Sheram ML, Laubach VE, Karlinsey MZ, Forbes MS, Macdonald T, Gaston B. S-Nitrosothiols signal hypoxia-mimetic vascular pathology. J Clin Invest 2007;117:2592–2601. [PubMed: 17786245]

38. Lachmanova V, Hnilickova O, Povysilova V, Hampl V, Herget J. N-Acetylcysteine inhibits hypoxic pulmonary hypertension most effectively in the initial phase of chronic hypoxia. Life Sci 2005;77:175–182. [PubMed: 15862602]

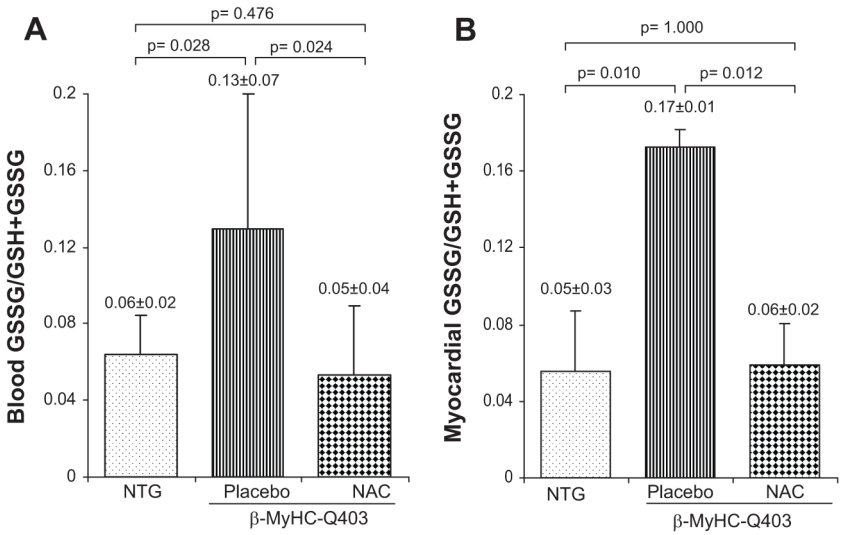

Figure 1.

Relative levels of oxidized to total glutathione (GSSG/GSH+GSSG). A and B show the ratio of oxidized to total glutathione in the blood (n = 6) and ventricular tissues (n = 3), respectively. GSSG/GSH+GSSG ratio was increased significantly in the blood and in the heart tissues in the *β*-MyHC-Q403 transgenic rabbits in the placebo group compared with nontransgenic (NTG) rabbits. In contrast, the ratio was normal in transgenic rabbits treated with NAC.

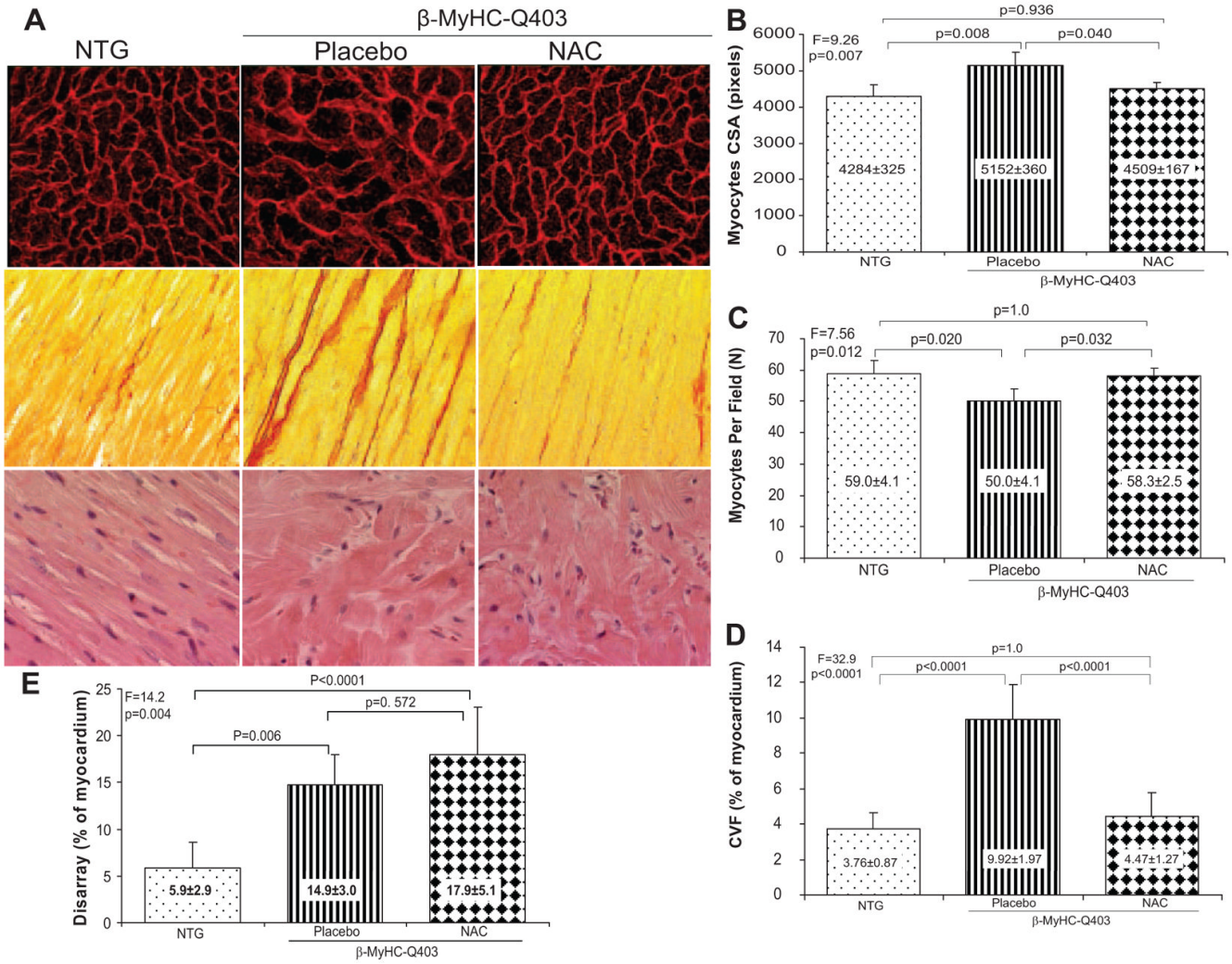

Figure 2.

Histological phenotype of myocyte hypertrophy (top panels), interstitial fibrosis (middle panels), and myocyte disarray (bottom panels). Representative high-magnification (×400) fields are shown (A). B through E show quantitative values of myocyte cross-sectional area (CSA), number of myocytes per each high-magnification (×400) microscopic field, CVF (% of myocardium), and extent of myocyte disarray (% of myocardium), respectively. NTG indicates nontransgenic.

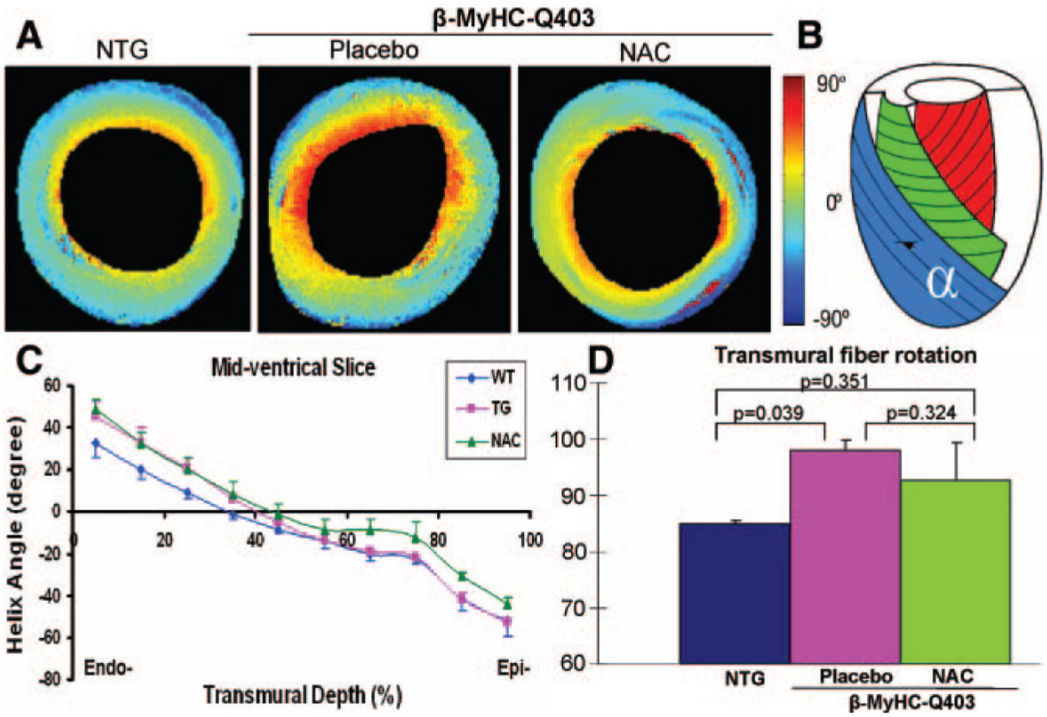

Figure 3.

Myofiber α-helical orientation as determined by diffusion-weighted (tensor) MRI. A, Representative cross-sectional images at mid ventricular levels are shown. Significant differences in myofiber orientation between transgenic rabbits in the placebo group and nontransgenic (NTG) rabbits at the endocardium and between the transgenic rabbits in the placebo and NAC groups at the epicardium are noted. B, Diagrammatic representation of myofiber α-helical orientation from epicardium to endocardium. C, Quantitative fiber orientation at mid ventricle is plotted against transmural depth from endocardium (Endo-) to epicardium (Epi-) to illustrate the differences among the 3 groups. WT indicates wild-type; TG, transgenic. D, Overall mean myofiber α-helical angles among the 3 groups.

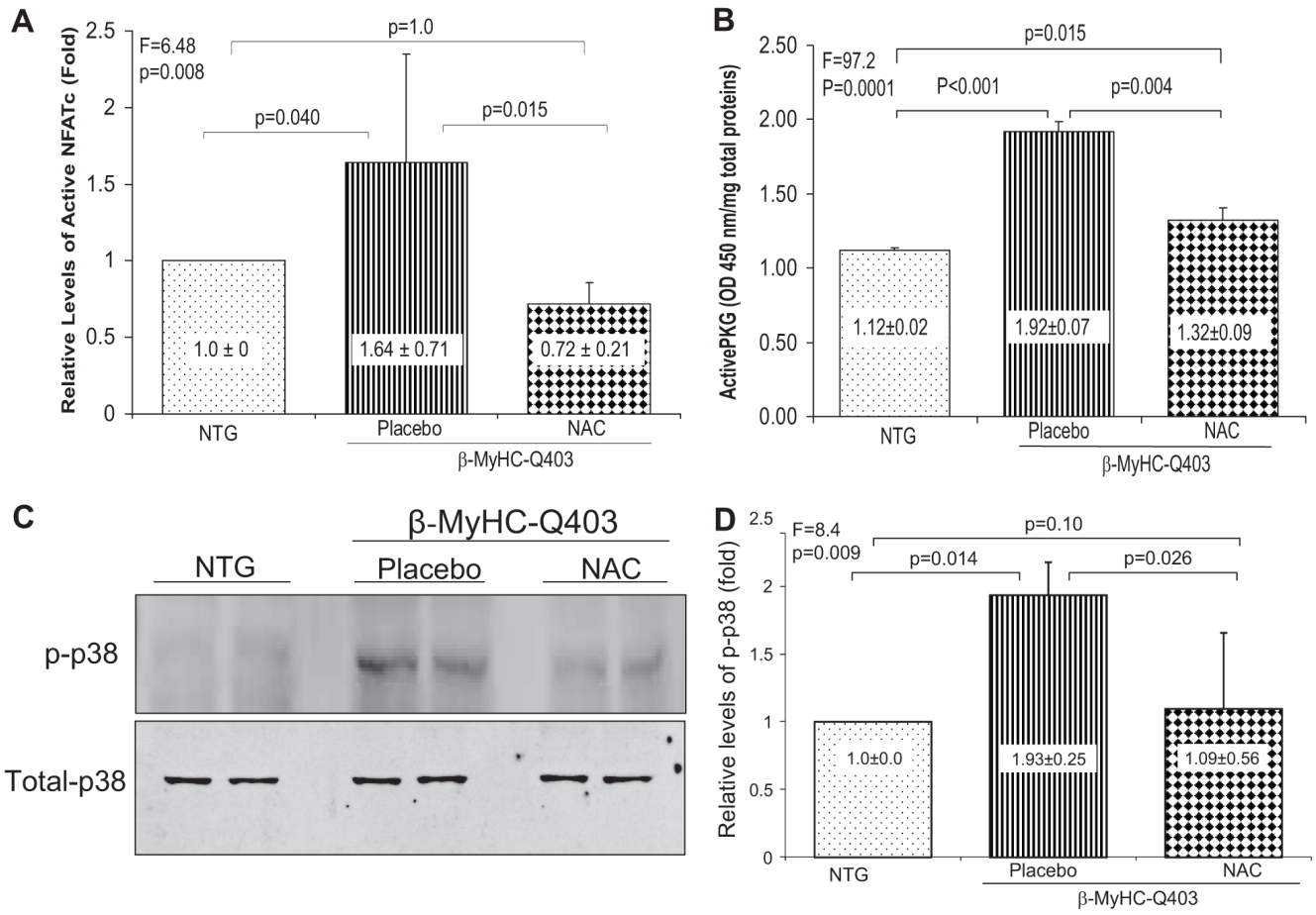

Figure 4.

Effects of NAC on myocardial levels of selective thio-sensitive molecules. A shows relative myocardial levels of active (dephosphorylated) NFATc1 normalized to that in the nontransgenic (NTG) rabbits. B shows myocardial levels of thiol-sensitive active PKG in the experimental groups. The upper blot in C shows phosphorylated p38 (p-p38) levels in the myocardium and the lower blot levels of total p38 levels, detected by immunoblotting. D shows quantitative levels of phospho-p38 as determined by densitometry and normalized to that in the nontransgenic group. In all panels, means and SDs are shown. The probability values at the top of each panel represent differences among the 3 groups. The Bonferroni adjusted probability values for paired groups are shown (n = 4 rabbits per group in each set of experiments).

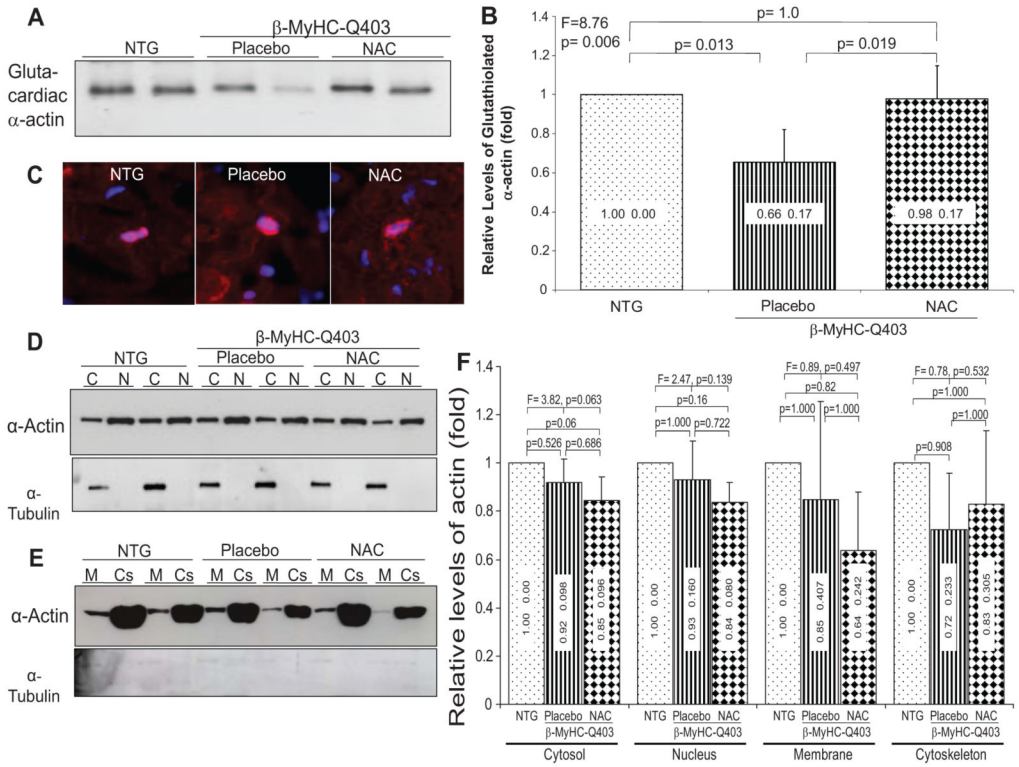

Figure 5.

Immunoblots showing levels of glutathiolated cardiac *α*-actin, detection of G-actin by immunofluorescence, and subcellular localization of *α*-actin. A, Coimmunoprecipitation of cardiac *α*-actin by a GSH antibody. B, Quantitative values of glutathiolated cardiac *α*-actin. C, Immunofluorescence staining of thin myocardial sections with DNase 1, a binding partner to G-actin, costained with DAPI (overlay pictures). D and E, Immunoblots of cardiac *α*-actin detected in subcellular compartments cytosolic (C), nuclear (N), membrane (M), and cytoskeletal (Cs). Panels showing expression levels of *α*-tubulin are shown to reflect comparability of loading conditions as well as purity of the extraction of subcellular proteins. F shows quantitative levels of cardiac *α*-actin in different cellular compartments. Means and SDs are shown. Comparisons among the 3 groups are shown at the top along with adjusted probability values for pairwise comparisons. NTG indicates nontransgenic.

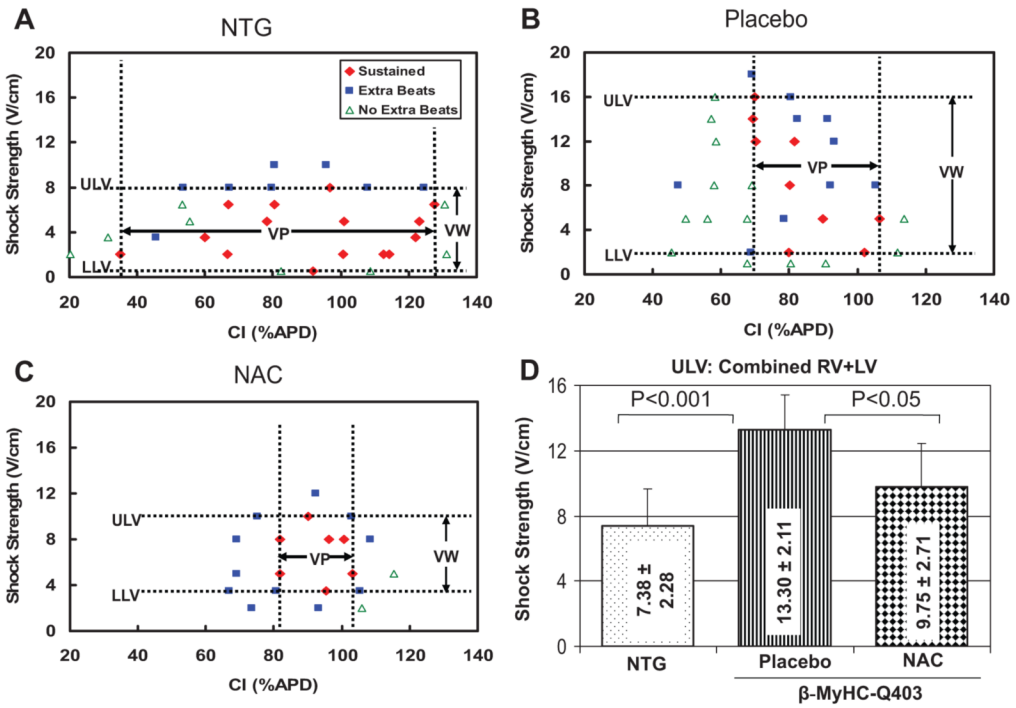

Figure 6.

Effects on vulnerable window and period. A through C show lower and upper limits of vulnerability (ULV) and the vulnerability window (VW) in nontransgenic (NTG), transgenic-placebo, and transgenic-NAC groups. LLV indicates lower limits of vulnerability; VP, vulnerable period; and APD, action potential duration. D, The mean values of combined right ventricular (RV) and LV ULV among the 3 groups. ULV in the placebo group is increased compared with nontransgenic rabbits. ULV and the vulnerable period were significantly lower in the NAC group (compared with the placebo group), indicating reduced susceptibility to shock-induced arrhythmias.

Table 1

Echocardiographic Phenotype at the Beginning (Baseline) and End of the 12-Month (Follow-up) Study

		β-MyHC-Q403		
	Nontransgenic	**Placebo**	**NAC**	***P***
n	10	10	10	…
IVST, mm				
Baseline	2.18±0.20	2.86±0.41	2.87±0.35	0.0002
Follow-up	2.10±0.16	3.14±0.38	2.14±0.22	<0.0001
Change	−0.08±0.31	0.28±0.48	−0.73±0.22	0.0001
P (paired *t* test)	0.219	0.049	<0.0001	
LVESD, mm				
Baseline	9.74±1.15	8.0±1.79	9.79±0.83	0.014
Follow-up	9.40±0.91	10.99±1.87	8.54±0.83	0.0007
Change	−0.336±1.43	2.99±2.67	−1.24±1.18	0.0002
P (paired *t* test)	0.250	0.008	0.010	
LV mass/body weight, g/kg				
Baseline	1.03±0.15 (1.02; 0.89–1.52)	1.30±0.56 (1.40; 1.05–1.71)	1.56±0.26 (1.63; 1.47–1.78)	0.002*
Follow-up	1.04±0.12 (1.0; 0.95–1.15)	1.80±0.64 (1.79; 1.21–2.02)	1.07±0.20 (1.10; 0.91–1.24)	0.003*
Change	0.01±0.16 (−0.05; −0.12–0.15)	0.50±0.69 (0.44; −0.04–1.04)	−0.49±0.21 (−0.46; −0.67–−0.36)	0.003*
P (paired *t* test)	0.425	0.023	0.0002	
LVFS, %				
Baseline	37.22±5.45	35.13±3.04	38.88±1.81	0.056
Follow-up	40.34±5.08	29.50±4.28	42.88±4.22	<0.0001
Change	3.12±9.0	−5.62±6.07	4.00±5.26	0.0221
P (paired *t* test)	0.166	0.017	0.034	
E/A				
Baseline	1.80±0.51	1.50±0.26	1.69±0.52	0.404
Follow-up	1.78±0.57	2.24±0.54	1.53±0.34	0.018
Change	−0.016±0.53	0.74±0.61	−0.17±0.45	0.003
P (paired *t* test)	0.467	0.002	0.167	
IVRT, ms				
Baseline	46.53±21.1	62.9±12.8	48.3±9.0	0.087
Follow-up	50.02±8.27	40.02±7.22	60.04±10.4	0.0004
Change	0.53±27.72 (0.0; −10.6–11.0)	−8.10±10.71 (5.50; 0.0–18.5)	15.46±40.11 (2.0; −14.1–53.0)	0.507*
P (paired *t* test)	0.201	0.020	0.151	

IVST indicates interventricular septal thickness; LVESD, LV end-systolic diameter; LVFS, LV fractional shortening; E/A, mitral valve inflow early to late velocities; and IVRT, isovolumic relaxation time.

* Median values were compared by Kruskal-Wallis test (median and quartile 1 to quartile 3 values are shown in parentheses).

Table 2

Upper Limits of Vulnerability and Vulnerable Period

	Nontransgenic		β-MyHC-Q403 Transgenic Rabbits			
			Placebo		NAC	
	RV	LV	RV	LV	RV	LV
Upper limits of vulnerability, V/cm	7.75±2.06	7.00±2.74	13.8±2.05*	12.80±2.28*	9.00±1.15†	10.5±3.79
Vulnerable period, % action potential duration						
Upper limit	114.4±17.4	111.7±17.6	110.0±8.9‡	95.8±7.0	102.6±4.0	98.4±8.1
Lower limit	43.3±24.0‖	50.8±21.4	62.9±14.6	51.5±17.1	82.5±7.9§	73.5±9.1§
Vulnerable period	71.1±41.1‖	60.9±33.8	47.2±21.3	48.2±25.5	20.1±5.7§	24.9±9.0

RV indicates right ventricle.

*$P<0.001$, nontransgenic vs placebo;

†$P<0.05$, placebo vs NAC.

‡$P<0.05$, nontransgenic vs placebo;

§$P<0.05$, placebo vs NAC;

‖$P<0.05$, nontransgenic vs NAC (pairwise P values corrected for multiple comparisons).